AIP | The Journal of Chemical Physics

Modelling non-adiabatic effects in H 3 + : Solution of the rovibrational Schrödinger equation with motion-dependent masses and mass surfaces

Edit Mátyus, Tamás Szidarovszky, and Attila G. Császár

Citation: The Journal of Chemical Physics **141**, 154111 (2014); doi: 10.1063/1.4897566
View online: http://dx.doi.org/10.1063/1.4897566
View Table of Contents: http://scitation.aip.org/content/aip/journal/jcp/141/15?ver=pdfcov
Published by the AIP Publishing

Modelling non-adiabatic effects in H_3^+: Solution of the rovibrational Schrödinger equation with motion-dependent masses and mass surfaces

Edit Mátyus,[1,a] Tamás Szidarovszky,[2] and Attila G. Császár[3,b]
[1]*Institute of Chemistry, Eötvös University, P.O. Box 32, H-1518 Budapest 112, Hungary*
[2]*MTA-ELTE Research Group on Complex Chemical Systems, Pázmány Péter sétány 1/A, H-1117 Budapest, Hungary*
[3]*Institute of Chemistry, Eötvös University, P.O. Box 32, H-1518, Budapest 112, Hungary and MTA-ELTE Research Group on Complex Chemical Systems, Pázmány Péter sétány 1/A, H-1117 Budapest, Hungary*

(Received 12 September 2014; accepted 30 September 2014; published online 20 October 2014)

Introducing different rotational and vibrational masses in the nuclear-motion Hamiltonian is a simple phenomenological way to model rovibrational non-adiabaticity. It is shown on the example of the molecular ion H_3^+, for which a global adiabatic potential energy surface accurate to better than 0.1 cm^{-1} exists [M. Pavanello, L. Adamowicz, A. Alijah, N. F. Zobov, I. I. Mizus, O. L. Polyansky, J. Tennyson, T. Szidarovszky, A. G. Császár, M. Berg *et al.*, Phys. Rev. Lett. **108**, 023002 (2012)], that the motion-dependent mass concept yields much more accurate rovibrational energy levels but, unusually, the results are dependent upon the choice of the embedding of the molecule-fixed frame. Correct degeneracies and an improved agreement with experimental data are obtained if an Eckart embedding corresponding to a reference structure of D_{3h} point-group symmetry is employed. The vibrational mass of the proton in H_3^+ is optimized by minimizing the root-mean-square (rms) deviation between the computed and recent high-accuracy experimental transitions. The best vibrational mass obtained is larger than the nuclear mass of the proton by approximately one third of an electron mass, $m_{\mathrm{opt,p}}^{(\mathrm{v})} = m_{\mathrm{nuc,p}} + 0.31224\ m_{\mathrm{e}}$. This optimized vibrational mass, along with a nuclear rotational mass, reduces the rms deviation of the experimental and computed rovibrational transitions by an order of magnitude. Finally, it is shown that an extension of the algorithm allowing the use of motion-dependent masses can deal with coordinate-dependent mass surfaces in the rovibrational Hamiltonian, as well. © *2014 AIP Publishing LLC*. [http://dx.doi.org/10.1063/1.4897566]

I. INTRODUCTION

Although in recent years pre-Born–Oppenheimer (BO) molecular structure theory[1–7] has made considerable advances, it remains a huge challenge to compute a large number of energy levels for even a small system such as the H_3^+ molecular ion when it is treated as a five-particle quantum system composed of electrons and protons. Thus, the central paradigm of computational high-resolution molecular spectroscopy of polyatomic and polyelectronic systems remains the solution of the time-independent nuclear-motion Schrödinger equation incorporating an adiabatic potential energy surface (PES) obtained from electronic structure theory.[8,9] The best rovibrational computations can challenge lower-resolution experiments[9] but there are also clear indications that to approach the accuracy of standard high-resolution experiments one needs to go beyond the commonly accepted approximations, i.e., not only beyond non-relativistic quantum mechanics[10] but also beyond the BO separation of the electronic and nuclear degrees of freedom. To wit, even if one has a global PES accurate to considerably better than 1 cm^{-1} in the complete configuration space considered, the rovibrational energy levels determined variationally with an exact kinetic energy operator (KEO) and this nearly "exact" PES may be inaccurate by up to several cm^{-1}.[11–13] These last remaining discrepancies between the ultimate adiabatic computational and the experimental rovibrational energy levels are due to the very nature of the BO separation of the electronic and nuclear degrees of freedom.

Thus, the next step of nuclear-motion theory toward true experimental accuracy is intrinsically connected to non-adiabatic "effects" and related corrections. Non-adiabatic perturbation theory (NAPT), developed for diatomic molecules,[14–16] has been successfully applied for the lowest-lying energy levels of the H_2 molecule and its deuterated isotopologues.[16–18] Furthermore, the NAPT-based dissociation energies of these four-particle systems, corrected for relativistic and quantum electrodynamics effects, agree within the stated uncertainties of the most accurate experiments.[17] In principle, it would be possible to extend NAPT to tri- and polyatomics but to the best of our knowledge only very limited efforts have been reported toward this goal.[19,20]

One feasible approach to move forward toward polyatomics considers the masses of the nuclei as motion-dependent variables. As an empirical and practical adoption of some of the results of NAPT on diatomics, second-order non-adiabatic corrections are described as "mass effects."[21,22] In particular, an increased vibrational mass, first suggested by Moss for the H_2^+ molecular ion,[23] where the rotational and vibrational terms are clearly separated in the

[a]Present address: Department of Chemistry, University of Cambridge, Lensfield Road, Cambridge CB2 1EW, United Kingdom. Electronic mail: matyus@chem.elte.hu.
[b]csaszar@chem.elte.hu

Hamiltonian, can be introduced to model some non-adiabatic effects also in triatomics. The corresponding slightly modified matrix elements for the Hamiltonian were derived by Polyansky and Tennyson[24] and the ensuing rovibrational Schrödinger equation was solved by them. This Moss-mass model, as it is often referred to, is an appealing choice for modelling non-adiabatic effects in polyatomic molecules because the correction appears to be conceptually relatively simple,[21] it keeps the notion of a PES almost intact, and it has been employed successfully to improve computed energy levels in relation to experiments.[11,24,25] Note that a further extension of this "motion-dependent mass" concept is the introduction of coordinate-dependent mass surfaces (CDMS) for both the rotational and vibrational masses.[21,22]

Motivated by these efforts and the corresponding useful results, we have considered the question how one could treat masses as variables in variational nuclear motion computations in the most general way for polyatomic cases. We believe no direct solution to this problem exists. The answer we provide is based on the extension of the fourth-age[26] quantum chemical code GENIUSH.[27,28] The GENIUSH protocol is based on a numerical construction of the kinetic energy operator and its matrix representation for the (quasi-)variational solution of the Schrödinger equation. This fully numerical approach allows us to solve the rovibrational Schrödinger equation using arbitrary internal coordinates, arbitrary embeddings, and arbitrary choices of reduced- and full-dimensional models of molecules. As shown here, the GENIUSH approach has one further advantage: with only a relatively minor modification of the existing computer code it is possible to include arbitrary vibrational and rotational masses and even coordinate-dependent mass surfaces in variational-type nuclear-motion computations of polyatomic systems.

II. SOLUTION OF THE ROVIBRATIONAL SCHRÖDINGER EQUATION WITH MOTION-DEPENDENT MASSES

A. The GENIUSH approach

The GENIUSH code solves the time-independent rovibrational Schrödinger equation

$$(\hat{T} + V)\Psi = E\Psi \tag{1}$$

with the potential energy surface V depending on the nuclear coordinates and the rovibrational kinetic energy operator written in a general form

$$\hat{T} = \frac{1}{2}\sum_{k=1}^{D+3}\sum_{l=1}^{D+3}\tilde{g}^{-1/4}\hat{p}_k G_{kl}\tilde{g}^{1/2}\hat{p}_l\tilde{g}^{-1/4} \tag{2}$$

$$= \frac{1}{2}\sum_{k=1}^{D}\sum_{l=1}^{D}\tilde{g}^{-1/4}\hat{p}_k G_{kl}\tilde{g}^{1/2}\hat{p}_l\tilde{g}^{-1/4}$$

$$+\frac{1}{2}\sum_{k=1}^{D}\sum_{a=1}^{3}(\tilde{g}^{-1/4}\hat{p}_k G_{k,D+a}\tilde{g}^{1/4}+\tilde{g}^{1/4}G_{k,D+a}\hat{p}_k\tilde{g}^{-1/4})\hat{J}_a$$

$$+\frac{1}{2}\sum_{a=1}^{3}G_{D+a,D+a}\hat{J}_a^2+\frac{1}{2}\sum_{a=1}^{3}\sum_{b>a}^{3}G_{D+a,D+b}[\hat{J}_a,\hat{J}_b]_+ \tag{3}$$

$$= \frac{1}{2}\sum_{k=1}^{D}\sum_{l=1}^{D}\tilde{g}^{-1/4}\hat{p}_k G_{kl}\tilde{g}^{1/2}\hat{p}_l\tilde{g}^{-1/4}$$

$$+\frac{1}{2}\sum_{k=1}^{D}\sum_{a=1}^{3}(\hat{p}_k G_{k,D+a}+G_{k,D+a}\hat{p}_k)\hat{J}_a$$

$$+\frac{1}{2}\sum_{a=1}^{3}G_{D+a,D+a}\hat{J}_a^2+\frac{1}{2}\sum_{a=1}^{3}\sum_{b>a}^{3}G_{D+a,D+b}[\hat{J}_a,\hat{J}_b]_+, \tag{4}$$

where the operators, in atomic units,

$$\hat{p}_k = -i\frac{\partial}{\partial q_k},\ k = 1,2,\ldots,D, \tag{5}$$

and

$$\hat{p}_{D+a} = -i\frac{\partial}{\partial \alpha_a} = \hat{J}_a,\ a = 1(x),2(y),3(z), \tag{6}$$

were inserted in the second equation corresponding to the $q_1, q_2, \ldots, q_D$ internal coordinates and the $\alpha_1, \alpha_2, \alpha_3$ orientational angles, respectively, and the volume element is $\mathrm{d}V = \mathrm{d}\alpha_1\mathrm{d}\alpha_2\mathrm{d}\alpha_3\mathrm{d}q_1\mathrm{d}q_2\ldots\mathrm{d}q_D$.[27,28] $[\hat{J}_a,\hat{J}_b]_+$ is the anticommutator of $\hat{J}_a$ and $\hat{J}_b$. If an N-particle system is treated in full vibrational dimensionality, then $D = 3N - 6$. We note that Eq. (3) is mathematically equivalent to the simpler form given in Eq. (4). If we consider the effect of the differential operators and remember that $\tilde{g}$ and G_{kl} depend only on the internal coordinates, we find that the $\tilde{g}$ coefficient remains only in the pure vibrational terms.

The central quantities $\boldsymbol{G} = \boldsymbol{g}^{-1} \in \mathbb{R}^{(D+3)\times(D+3)}$ and $\tilde{g} = \det \boldsymbol{g}$ are defined as

$$g_{kl} = \sum_{i=1}^{N} m_i \boldsymbol{t}_{ik}^{\mathrm{T}}\boldsymbol{t}_{il},\quad k,l = 1,2,\ldots,D+3, \tag{7}$$

with the vibrational and rotational **t**-vectors

$$\boldsymbol{t}_{ik} = \frac{\partial \boldsymbol{r}_i}{\partial q_k} \in \mathbb{R}^3,\quad i = 1,2,\ldots,N,\ k = 1,2,\ldots,D \tag{8}$$

and

$$\boldsymbol{t}_{i,D+a} = \boldsymbol{e}_a \times \boldsymbol{r}_i \in \mathbb{R}^3,\quad i = 1,2,\ldots,N,\ a = 1(x),2(y),3(z), \tag{9}$$

respectively, whereby $\boldsymbol{e}_a$ is a unit vector pointing toward the a axis of the chosen embedding and $\boldsymbol{r}_i$ corresponds to the position vector of the ith nucleus in this embedding (the center of mass is at the origin).

In GENIUSH, this general formulation is implemented in a quasi-variational procedure using discrete variable representation (DVR) for the internal degrees of freedom, Wang functions for the rotational part, a numerical construction for the kinetic energy terms over the DVR grid, and a Lanczos iterative eigensolver for the solution of the vibrational[27] and rovibrational[28] Schrödinger equation of the atomic nuclei.

B. Implementation of the motion-dependent mass concept

In the rigorous derivation of NAPT developed for diatomics,[15,16] two coordinate-dependent coefficients appear.

These coefficients have been identified as special vibrational and rotational masses, which are coordinate dependent, and are associated with the vibrational and the rotational terms of the kinetic energy operator (there is no rovibrational term in the case of a diatomic molecule). The earliest practical adoption of this result to polyatomics, in fact for triatomic H_3^+, was made by Polyansky and Tennyson.[24] For simplicity, they used constant masses: Moss' mass[23] was written into the vibration-only term of the kinetic energy operator, while the nuclear mass was used in all the operator terms containing the rotational angular momentum operators, i.e., in the rotational and rovibrational terms.

The GENIUSH approach allows the straightforward implementation of the above non-adiabatic model. The Hamiltonian in Eq. (4) is adapted as follows:

$$\begin{aligned}\hat{\mathcal{T}} = &\frac{1}{2}\sum_{k=1}^{D}\sum_{l=1}^{D}(\tilde{g}^{(\mathrm{v})})^{-1/4}\hat{p}_k G^{(\mathrm{v})}_{kl}(\tilde{g}^{(\mathrm{v})})^{1/2}\hat{p}_l(\tilde{g}^{(\mathrm{v})})^{-1/4}\\ &+\frac{1}{2}\sum_{k=1}^{D}\sum_{a=1}^{3}\left(\hat{p}_k G^{(\mathrm{r})}_{k,D+a}+G^{(\mathrm{r})}_{k,D+a}\hat{p}_k\right)\hat{J}_a\\ &+\frac{1}{2}\sum_{a=1}^{3}G^{(\mathrm{r})}_{D+a,D+a}\hat{J}_a^2+\frac{1}{2}\sum_{a=1}^{3}\sum_{b>a}^{3}G^{(\mathrm{r})}_{D+a,D+b}[\hat{J}_a,\hat{J}_b]_+,\end{aligned} \tag{10}$$

where the symbol $\hat{\mathcal{T}}$ is used instead of $\hat{T}$ to indicate the difference introduced by the use of motion-dependent masses. Superscripts (v) and (r) indicate that the quantity is evaluated with the vibrational and the rotational mass, respectively. The $\boldsymbol{G}^{(\mathrm{v})} = (\boldsymbol{g}^{(\mathrm{v})})^{-1}$ matrix is constructed with the vibrational masses, $\boldsymbol{m}^{(\mathrm{v})} = (m_1^{(\mathrm{v})}, \ldots, m_N^{(\mathrm{v})})$, and can be written into blocks

$$\boldsymbol{G}^{(\mathrm{v})}(\boldsymbol{q};\boldsymbol{m}^{(\mathrm{v})}) = \left(\begin{array}{c|c}\boldsymbol{G}^{(\mathrm{v})}_{(1:D,1:D)} & \boldsymbol{G}^{(\mathrm{v})}_{(1:D,D+1:D+3)}\\ \hline \boldsymbol{G}^{(\mathrm{v})}_{(D+1:D+3,1:D)} & \boldsymbol{G}^{(\mathrm{v})}_{(D+1:D+3,D+1:D+3)}\end{array}\right) \times \in \mathbb{R}^{(D+3)\times(D+3)} \tag{11}$$

with $\tilde{g}^{(\mathrm{v})} = \det\boldsymbol{g}^{(\mathrm{v})}$. Similarly, the $\boldsymbol{G}^{(\mathrm{r})} = (\boldsymbol{g}^{(\mathrm{r})})^{-1}$ matrix is evaluated with the rotational masses, $\boldsymbol{m}^{(\mathrm{r})} = (m_1^{(\mathrm{r})}, \ldots, m_N^{(\mathrm{r})})$, and the corresponding block form is

$$\boldsymbol{G}^{(\mathrm{r})}(\boldsymbol{q};\boldsymbol{m}^{(\mathrm{r})}) = \left(\begin{array}{c|c}\boldsymbol{G}^{(\mathrm{r})}_{(1:D,1:D)} & \boldsymbol{G}^{(\mathrm{r})}_{(1:D,D+1:D+3)}\\ \hline \boldsymbol{G}^{(\mathrm{r})}_{(D+1:D+3,1:D)} & \boldsymbol{G}^{(\mathrm{r})}_{(D+1:D+3,D+1:D+3)}\end{array}\right) \times \in \mathbb{R}^{(D+3)\times(D+3)}. \tag{12}$$

Next, we introduce the compact notation

$$\boldsymbol{\mathcal{G}}(\boldsymbol{q};\boldsymbol{m}^{(\mathrm{v})},\boldsymbol{m}^{(\mathrm{r})}) = \left(\begin{array}{c|c}\boldsymbol{G}^{(\mathrm{v})}_{(1:D,1:D)} & \boldsymbol{G}^{(\mathrm{r})}_{(1:D,D+1:D+3)}\\ \hline \boldsymbol{G}^{(\mathrm{r})}_{(D+1:D+3,1:D)} & \boldsymbol{G}^{(\mathrm{r})}_{(D+1:D+3,D+1:D+3)}\end{array}\right) \times \in \mathbb{R}^{(D+3)\times(D+3)}, \tag{13}$$

where the upper left (pure vibrational) block contains the pure vibrational block of $\boldsymbol{G}^{(\mathrm{v})}$, while the other three blocks are taken over from the corresponding blocks of $\boldsymbol{G}^{(\mathrm{r})}$.

Then, using this notation

$$\begin{aligned}\hat{\mathcal{T}} = &\frac{1}{2}\sum_{k=1}^{D}\sum_{l=1}^{D}(\tilde{g}^{(\mathrm{v})})^{-1/4}\hat{p}_k\mathcal{G}_{kl}(\tilde{g}^{(\mathrm{v})})^{1/2}\hat{p}_l(\tilde{g}^{(\mathrm{v})})^{-1/4}\\ &+\frac{1}{2}\sum_{k=1}^{D}\sum_{a=1}^{3}\left(\hat{p}_k\mathcal{G}_{k,D+a}+\mathcal{G}_{k,D+a}\hat{p}_k\right)\hat{J}_a\\ &+\frac{1}{2}\sum_{a=1}^{3}\mathcal{G}_{D+a,D+a}\hat{J}_a^2+\frac{1}{2}\sum_{a=1}^{3}\sum_{b>a}^{3}\mathcal{G}_{D+a,D+b}[\hat{J}_a,\hat{J}_b]_+.\end{aligned} \tag{14}$$

In the GENIUSH code, the coefficients of the differential operators appearing in the kinetic energy operator are computed at every grid point, so for the non-adiabatic version the quantities $\{\boldsymbol{g}^{(\mathrm{v})}, \boldsymbol{G}^{(\mathrm{v})}, \tilde{g}^{(\mathrm{v})}\}$ and $\{\boldsymbol{g}^{(\mathrm{r})}, \boldsymbol{G}^{(\mathrm{r})}\}$ are evaluated at each and every grid point. The vibrational **t**-vectors are computed by numerical differentiation using the central difference formula and increased precision arithmetics (quadruple precision in Fortran). The numerical values of the matrix $\boldsymbol{\mathcal{G}} \in \mathbb{R}^{(D+3)\times(D+3)}$ and the real values $\tilde{g}^{(\mathrm{v})}$ are stored at every grid point and used in the matrix-vector multiplication to compute eigenvalues and eigenvectors with a Lanczos algorithm. All eigenvalues and eigenvectors corresponding to a selected J value are computed in a single run irrespective of their symmetry characteristics.

III. NUMERICAL RESULTS FOR H_3^+

Rovibrational computations have been carried out for the H_3^+ molecular ion with the extended GENIUSH code and using the highly accurate adiabatic GLH3P potential energy surface.[11,12] The rotational mass was the nuclear mass of the proton, $m_{\mathrm{p}}^{(\mathrm{r})} = 1.0072765\ \mathrm{u} = 1836.1522\ m_{\mathrm{e}}$, while the vibrational mass was first chosen to be the Moss mass, $m_{\mathrm{p}}^{(\mathrm{v})} = 1.0075372\ \mathrm{u} = 1836.6275\ m_{\mathrm{e}}$. Additional conversion factors used throughout the computations are $1\,\mathrm{cm}^{-1} = 219\,474.63\ E_{\mathrm{h}}$ and $1\ \mathrm{u} = 1822.8880\,m_{\mathrm{e}}$.

A. Embedding dependence of the computed non-adiabatic rovibrational energy levels

In the first set of computations with the newly extended GENIUSH code, we used valence-type vibrational coordinates (r_1, r_2, $\cos\theta$) and an "*xxy*" bond-vector embedding.[38] The matrix representation for the kinetic and potential energy operators was built on a direct-product grid constructed from potential-optimized DVR (PO-DVR)[29–31] points for the r_1 and r_2 stretch-type coordinates and Legendre-DVR for $\cos\theta$.

The rovibrational energies were carefully converged with respect to the coordinate intervals and the grid size: 30 PO-DVR points optimized over 100 primitive Hermite-DVR points scaled to the $r_1, r_2 \in [0.1, 5.0]$ bohr interval and 60 (unscaled) Legendre DVR points were used. For the increased-precision numerical differentiation, the step-size was 10^{-5} a.u.[27] and the computed energy levels were found to be stable with respect to small changes of this parameter.

The GENIUSH results obtained were checked against independent variational results obtained with the D^{2}FOPI

code[32] using Jacobi coordinates as internal coordinates and a bond-vector embedding. Unlike GENIUSH, D^{2}FOPI does take advantage of the symmetry of the nuclear motion problem. Perfect agreement was found between the precise results of the two independent computations.

In spite of all the extensive numerical efforts, we have observed a sizeable splitting, larger than 0.001 cm^{-1}, for certain rovibrational ($J > 0$) energy levels which should have been obtained as degenerate pairs. After a very careful check of the GENIUSH implementation and the parameter selection, we have considered other possible internal coordinates and more importantly, other possible embeddings of the body-fixed frame, as a potential reason for this artificial corruption of the permutational symmetry manifested in the rovibrational energy levels. The universality and flexibility of the GENIUSH approach allows straightforward switching among different embeddings.[28,33] As an alternative to the *xxy* embedding, we used the bisector embedding, an Eckart embedding corresponding to a reference structure of C_{2v} point-group symmetry (henceforth called Eckart(C_{2v})), as well as an Eckart embedding corresponding to a D_{3h} reference structure (henceforth called Eckart(D_{3h})). Artificial splittings of certain degenerate rovibrational energy levels occurred in all cases except for Eckart(D_{3h}).

In Figure 1, the effect of the various selected embeddings on the rovibrational energy levels, $J = 1 - 5$, is presented corresponding to the lowest-energy vibrational level, 00^0 (the numerical results used to generate this Figure are deposited in the supplementary material[34]). We note that in Fig. 1 both degenerate energy levels are plotted, and thus any artificial splitting can be observed. The reference values are obtained with Eckart(D_{3h}), which reproduces the expected degeneracies perfectly. It is apparent from the results obtained that the application of a bisector (or an Eckart(C_{2v})) embedding improves the results of the *xxy* embedding. Nevertheless, the correct degeneracies and the best agreement with the experimental results[13,35–37] are obtained when an Eckart embedding corresponding to a D_{3h} reference structure is used. Deviation from the Eckart(D_{3h}) results increases with J and depends also on the value of the G label of the energy levels[13,35] (Fig. 1).

It is common knowledge in computational molecular spectroscopy that vibration-only eigenvalues are insensitive to the embedding chosen to represent the rovibrational kinetic energy operator. More precisely, although convergence of the rovibrational energy values does depend on the embedding, the converged results should be embedding independent. This is the case in spite of the fact that the mathematical form of most of the rovibrational Hamiltonians is not permutationally invariant. As shown here for the case of H_3^+, if motion-dependent masses are employed in the kinetic energy operator, as explained in Sec. II, the rovibrational eigenvalues become embedding dependent. The best agreement with experiment and the best connection with the adiabatic computations (using the same mass for the different types of motion), e.g., degeneracy of rovibrational levels, is obtained if the Eckart(D_{3h}) embedding is employed. These observations hold for rovibrational levels corresponding to either the ground or excited vibrational states.

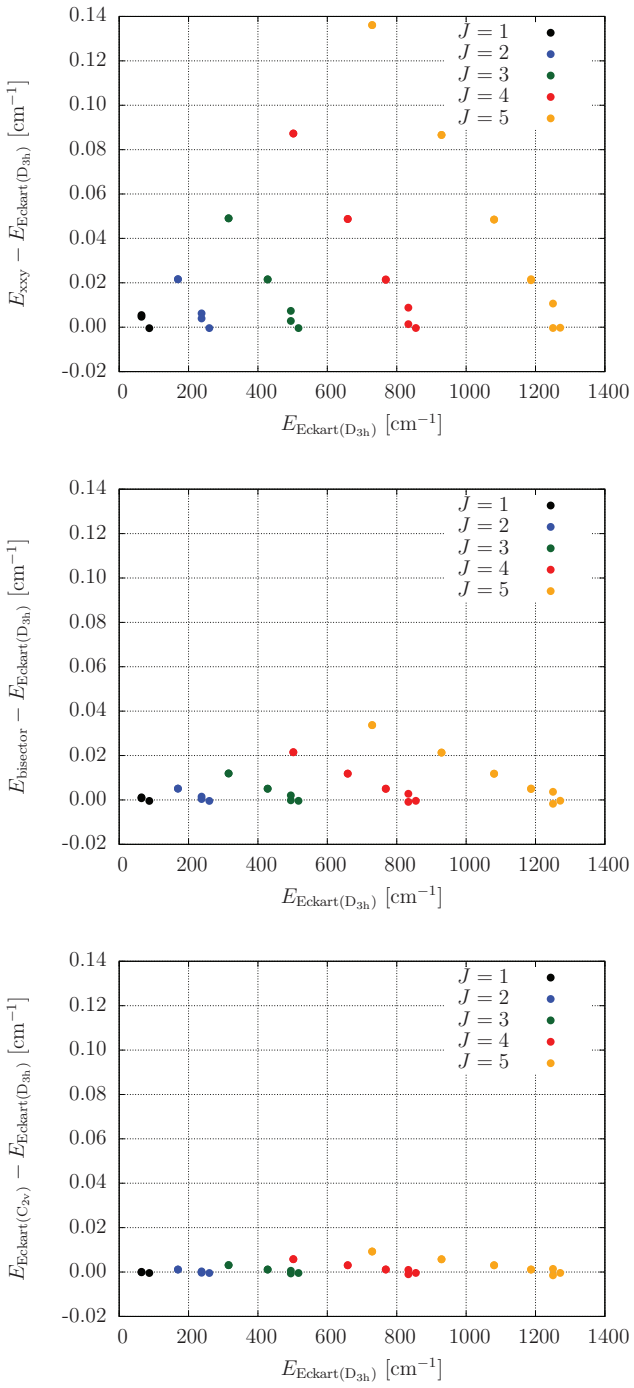

FIG. 1. Deviation of the rovibrational energy levels of H_3^+ corresponding to the lowest vibrational state, 00^0, obtained with different embeddings of the body-fixed frame and the non-adiabatic extension of the GENIUSH code (the definition of the embeddings is given in the text). In the computations, the rotational mass was the nuclear mass of the proton, $m_{\mathrm{p}}^{(\mathrm{r})} = 1.0072765$ u, while the vibrational mass was the Moss mass, $m_{\mathrm{p}}^{(\mathrm{v})} = 1.0075372$ u.

We explain the special role of the Eckart(D_{3h}) embedding in these computations as follows. Although most of the molecular Hamiltonians used in practice have a mathematical form which is non-invariant to the permutation of identical nuclei, they are mathematically equivalent with a translationally invariant (TI) Hamiltonian (written in translationally invariant Cartesian coordinates) if the rotational and vibrational

masses are the same. It is easy to see that this TI Hamiltonian satisfies the permutational symmetry of identical nuclei, and thus the proper degeneracy pattern of the computed rovibrational levels is guaranteed. If we write in some rotational mass in the rotational and rovibrational terms and some vibrational mass (different from the rotational mass) in the vibrational terms of the Hamiltonian according to Sec. II, than we lose any direct connection with a TI Hamiltonian. Thus, it cannot be guaranteed that the expected degeneracy of the computed rovibrational levels is maintained. The Eckart(D_{3h}) Hamiltonian is special in the case of H_3^+ because the three protons enter the definition of the body-fixed frame equivalently, and thus we can say that this embedding is permutationally invariant. Then, the rotational, the rovibrational, and the vibrational terms are independently permutationally invariant (if we assume first that we have permutationally invariant internal coordinates). So, we can use the different rotational and vibrational masses in the Hamiltonian according to the common recipe, the resulting Hamiltonian remains permutationally invariant, and thus we can expect that the computed eigenvalues have the proper degeneracy. Since we use the same mass for the internal degrees of freedom, we are free to switch between different internal coordinates, and thus the permutational invariance condition for the internal coordinates is not necessary.

B. The optimal vibrational mass for H_3^+

Moss determined the optimal vibrational mass of the proton for the hydrogen molecular ion, H_2^+, which is $m^{(v)}_{\mathrm{Moss,p}} = m_{\mathrm{nuc,p}} + 0.47531\ m_e$.[23] At the same time, he noted that there was no definitive reason for using a rotational mass different from the nuclear mass. This vibrational mass, thus originally determined for H_2^+, has become known as the Moss mass for the proton and was later successfully transferred for the computation of rovibrational energy levels of H_3^+,[11,24] while the rotational mass was the nuclear mass according to Moss' recipe for H_2^+.[23] Although it was noted already in Ref. 24 that even better agreement with experiment can be obtained by adjusting the vibrational mass, this was not attempted there.

In this section, we use the non-adiabatic version of the GENIUSH program and determine the optimal vibrational mass for the proton of H_3^+ by minimizing the root-mean-squared (rms) deviation between the computed and the most recent experimental transitions.[36,37] The rms deviation for the 15 observed and computed transitions using different vibrational masses is shown in Figure 2. Fig. 2 shows that there is a well-defined minimum corresponding to the optimal mass, $m^{(v)}_{\mathrm{opt,p}} = m_{\mathrm{nuc,p}} + 0.31224\ m_e$. The full list of experimental transitions used in our work and the deviations of the computed rovibrational energy levels obtained with the nuclear mass, the Moss mass, and our optimized mass is given in Table I (the computed energy levels used for this table are deposited in the supplementary material[34]). It is apparent that whereas the replacement of the vibrational nuclear mass with Moss' mass reduces the rms deviation only by a factor of 2, the optimization of the vibrational mass provides more than an order of magnitude improvement.

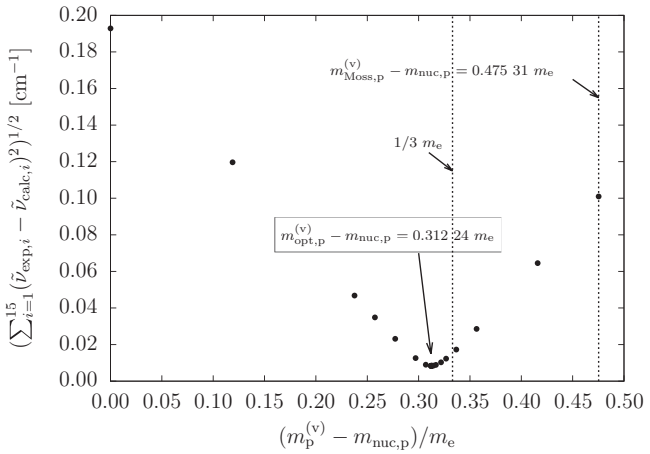

FIG. 2. Optimization of the vibrational mass for the proton with respect to 15 recently obtained high-accuracy experimental rovibrational transitions[36,37] connecting the two lowest-energy vibrational states of H_3^+, 00^0 and 01^1. The non-adiabatic computations were carried out with the GENIUSH program using motion-dependent masses and an Eckart embedding with a reference structure of D_{3h} point-group symmetry. The rotational mass was the nuclear mass of the proton, $m_p^{(r)} = 1.0072765$ u, throughout the computations.

To understand the qualitative meaning of the numerical result obtained, we first note that the optimal mass for H_3^+ is larger than the nuclear mass of the proton by about 1/3 of an electron mass. Interestingly, it is significantly smaller than the Moss mass obtained for H_2^+, which is larger than the nuclear mass by about 1/2 of an electron mass. Now, remembering the expressive explanation of second-order non-adiabatic corrections, according to which the electrons "follow the nuclei" and hence increase their effective mass, our result might first appear to be counter-intuitive for an assembly of two electrons and three protons. The puzzle is quickly resolved with the help of a recent work by Diniz *et al.*,[22] in which a core-mass surface was derived from a simple Mulliken population analysis carried out for H_3^+. Using this mass surface the authors determined effective masses for each vibrational state in an iterative procedure, and they obtained, for example, $m_p^{(v)} = m_{\mathrm{nuc,p}} + 0.3155\ m_e$ for the 00^0 and $m_p^{(v)} = m_{\mathrm{nuc,p}} + 0.3189\ m_e$ for the 01^1 vibrational state. These results are in excellent agreement with our vibrational mass optimized with respect to the most recent experimental transitions including these two vibrational states.

IV. SOLUTION OF THE ROVIBRATIONAL SCHRÖDINGER EQUATION WITH COORDINATE-DEPENDENT MASS SURFACES

The recent development[22] of rotational and vibrational mass surfaces for H_3^+ calls for the direct solution of the rovibrational Schrödinger equation including the full mass surfaces, instead of having to rely on iterative solutions as in Ref. 22.

One of the principal ideas underlying the GENIUSH protocol is the grid representation of not only the PES but also the coefficients of the differential operators in the KEO. The coefficients of the KEO are evaluated on a grid without the explicit knowledge of their analytic form. With this idea in mind,

TABLE I. Comparison of experimental and computed rovibrational transitions, in cm^{-1}, of H_3^+. The computed transitions were obtained with the GENIUSH program accounting for rovibrational non-adiabatic effects. The nuclear mass of the proton was $m_{nuc,p} = 1.0072765\,u = 1836.1522\,m_e$.

$v_1 v_2^{\lvert l\rvert}, (J, G)\{u/l/m\}$[a]				$\tilde{\nu}_{Exp}$[b]	$\Delta\tilde{\nu}$(nuc)[c]	$\Delta\tilde{\nu}$(vibopt)[d]	$\Delta\tilde{\nu}$(Moss)[e]
01^1	(4,3)u	00^0	(3,3)m	2918.026	−0.203	−0.006	0.097
01^1	(5,4)l	00^0	(4,4)m	2894.490	−0.204	−0.016	0.082
01^1	(4,2)l	00^0	(3,2)m	2832.196	−0.195	−0.006	0.093
01^1	(4,3)l	00^0	(3,3)m	2829.925	−0.199	−0.010	0.089
01^1	(3,1)u	00^0	(2,1)m	2826.117	−0.201	−0.005	0.097
01^1	(3,2)u	00^0	(2,2)m	2823.138	−0.198	−0.003	0.100
01^1	(3,1)l	00^0	(2,1)m	2765.544	−0.193	−0.002	0.098
01^1	(3,2)l	00^0	(2,2)m	2762.070	−0.195	−0.004	0.095
01^1	(2,1)u	00^0	(1,1)m	2726.220	−0.193	0.002	0.103
01^1	(2,0)m	00^0	(1,0)m	2725.898	−0.195	0.000	0.101
01^1	(2,1)l	00^0	(1,1)m	2691.443	−0.190	0.001	0.101
01^1	(2,2)m	00^0	(2,2)m	2554.666	−0.181	0.013	0.115
01^1	(1,1)m	00^0	(1,1)m	2545.420	−0.181	0.013	0.114
01^1	(1,0)m	00^0	(1,0)m	2529.725	−0.181	0.011	0.112
01^1	(2,1)l	00^0	(2,1)m	2518.212	−0.181	0.011	0.111
rms[f]					0.193[c]	0.008[d]	0.101[e]

[a]Vibrational and rotational labels of the upper and lower rovibrational states involved in the transitions, taken from Refs. 36 and 37. The labels are clearly explained in Ref. 13.

[b]Experimental transitions taken from Refs. 36 and 37. If the same transition was available from both experiments, the average of the two measurements was used.

[c]$\Delta\tilde{\nu}(\text{nuc}) = \tilde{\nu}_{Exp} - \tilde{\nu}(\text{nuc})$, where $\tilde{\nu}$(nuc) was computed using the nuclear mass for both the vibrational and the rotational mass, $m_p^{(v)} = m_p^{(r)} = m_{nuc,p}$.

[d]$\Delta\tilde{\nu}(\text{vibopt}) = \tilde{\nu}_{Exp} - \tilde{\nu}(\text{vibopt})$, where $\tilde{\nu}$(vibopt) was computed using the optimized vibrational mass (see the text and Figure 2), $m_p^{(v)} = m_{opt,p}^{(v)} = m_{nuc,p} + 0.312\,24\,m_e$, and the rotational mass was the nuclear mass of the proton, $m_p^{(r)} = m_{nuc,p}$.

[e]$\Delta\tilde{\nu}(\text{Moss}) = \tilde{\nu}_{Exp} - \tilde{\nu}(\text{Moss})$, where $\tilde{\nu}$(Moss) was computed using the Moss mass[23] for the vibrational mass, $m_p^{(v)} = m_{Moss,p}^{(v)} = m_{nuc,p} + 0.475\,31\,m_e$, and the rotational mass was the nuclear mass of the proton, $m_p^{(r)} = m_{nuc,p}$.

[f]rms is the root-mean-squared deviation of the experimental and computed transitions.

the implementation of CDMS in the GENIUSH program is almost straightforward and the major aspects are summarized in this section.

The central quantity in our treatment is the rovibrational $\boldsymbol{g}$ matrix, which is now evaluated with the internal-coordinate-dependent masses, $m_i(\boldsymbol{q})$, and the vibrational and rotational **t**-vectors

$$g_{kl} = \sum_{i=1}^{N} m_i(\boldsymbol{q}) \boldsymbol{t}_{ik}^{\mathrm{T}} \boldsymbol{t}_{il}, \quad k, l = 1, 2, \ldots, D+3. \tag{15}$$

It is important to remember that the vibrational and rotational **t**-vectors are defined as

$$\boldsymbol{t}_{ik} = \frac{\partial \boldsymbol{r}_i}{\partial q_k} \in \mathbb{R}^3, \quad i = 1, 2, \ldots, N, \; k = 1, 2, \ldots, D \tag{16}$$

and

$$\boldsymbol{t}_{i,D+a} = \boldsymbol{e}_a \times \boldsymbol{r}_i \in \mathbb{R}^3, \quad i = 1, 2, \ldots, N, \; a = 1(x), 2(y), 3(z), \tag{17}$$

respectively, and that $\boldsymbol{r}_i$ is the translationally invariant Cartesian coordinate of the ith atomic nucleus expressed in the body-fixed frame.

Even if the orientation of the body-fixed frame is not dependent on the masses, its origin is at the center of mass of the nuclei, and thus the mass surface enters the expression

$$\boldsymbol{r}_i(\boldsymbol{q}, \boldsymbol{m}(\boldsymbol{q})) = \boldsymbol{\rho}_i(\boldsymbol{q}) - \frac{1}{M(\boldsymbol{q})} \sum_{k=1}^{N} m_k(\boldsymbol{q}) \boldsymbol{\rho}_k(\boldsymbol{q}), \quad i = 1, 2, \ldots, N, \tag{18}$$

where $M(\boldsymbol{q}) = \sum_{j=1}^{N} m_j(\boldsymbol{q})$ and $\boldsymbol{\rho}_i$ denotes the Cartesian coordinates of the ith nucleus in a frame which has axes parallel to the axes of the body-fixed frame, but its origin is not at the center of mass. If analytic first derivatives of the mass function, $\partial m_k / \partial q_n$, are available, then the vibrational **t**-vectors can be calculated as

$$\boldsymbol{t}_{in} = \frac{\partial}{\partial q_n} \left(\boldsymbol{\rho}_i(\boldsymbol{q}) - \frac{1}{M(\boldsymbol{q})} \sum_{k=1}^{N} m_k(\boldsymbol{q}) \boldsymbol{\rho}_k(\boldsymbol{q}) \right) \tag{19}$$

$$= \frac{\partial \boldsymbol{\rho}_i}{\partial q_n} - \frac{1}{M} \sum_{k=1}^{N} \left(\frac{\partial m_k}{\partial q_n} (\boldsymbol{\rho}_k - \boldsymbol{\rho}_{\mathrm{COM}}) + m_k \frac{\partial \boldsymbol{\rho}_k}{\partial q_n} \right), \tag{20}$$

with $\boldsymbol{\rho}_{\mathrm{COM}} = \sum_{j=1}^{N} m_j(\boldsymbol{q}) / M(\boldsymbol{q}) \boldsymbol{\rho}_j$. Otherwise, the derivative is calculated by finite differences and the accuracy and stability must be carefully tested. It might be necessary to call the mass function with increased arithmetic precision (quadruple precision in Fortran). In the special case of identical nuclei, i.e., atomic nuclei described with equal coordinate-dependent masses for any internal structure (see Ref. 22 for an interesting discussion of identical or non-identical coordinate-dependent masses for H_3^+), $m_1(\boldsymbol{q})$

$= m_2(\boldsymbol{q}) = \ldots = m_N(\boldsymbol{q}) =: m(\boldsymbol{q})$, it is useful to note that Eq. (18) simplifies to

$$\boldsymbol{r}_i(\boldsymbol{q}, \boldsymbol{m}(\boldsymbol{q})) = \boldsymbol{\rho}_i(\boldsymbol{q}) - \frac{1}{Nm(\boldsymbol{q})} \sum_{k=1}^{N} m(\boldsymbol{q}) \boldsymbol{\rho}_k(\boldsymbol{q})$$

$$= \boldsymbol{\rho}_i(\boldsymbol{q}) - \frac{1}{N} \sum_{k=1}^{N} \boldsymbol{\rho}_k(\boldsymbol{q}). \quad (21)$$

Thus, the coordinate dependence of the masses does not enter the vibrational **t**-vectors in this special case. In general, the orientation of the body-fixed frame can depend on the masses, and then it is probably best to calculate the vibrational **t**-vectors by calling the mass surfaces using increased arithmetic precision.

Once the rotational and vibrational **t**-vectors have been calculated considering the coordinate-dependent mass surfaces, the approach is identical with the one explained for the case of constant but motion-dependent masses. The rovibrational $\boldsymbol{g}^{(\mathrm{r})}$ and $\boldsymbol{g}^{(\mathrm{v})}$ matrices are evaluated at every quadrature point using the corresponding values of the rotational and vibrational mass surfaces, $\boldsymbol{m}^{(\mathrm{r})}(\boldsymbol{q})$ and $\boldsymbol{m}^{(\mathrm{v})}(\boldsymbol{q})$, respectively. Then, the hybrid $\mathcal{G}$ matrix is constructed according to Eq. (13), and by remembering that $\tilde{g}^{(v)} = \det \boldsymbol{g}^{(\mathrm{v})}$ the kinetic energy operator is defined similar to Eq. (14).

The observations made for the motion-dependent but constant masses should also certainly be fulfilled for any application of motion-dependent and coordinate-dependent mass surfaces. For identical nuclei, e.g., H_3^+ or D_3^+, we would use an embedding which respects the permutational symmetry of the nuclei. It is now left for further consideration if it is sufficient to define the orientation of such a permutationally invariant frame without having to rely on the coordinate-dependent masses or if the full inclusion of the coordinate-dependent mass surface is practical or necessary.

V. OUTLOOK

We can think of at least two important questions which remained unanswered in this study and left for future work. First, one might ask if we can have a "paper-and-pencil" demonstration for the embedding dependence of the computed rovibrational energy levels. Such a demonstration is probably possible, but it comes with the difficulty that one has to state something about the computed energy levels while changing a parameter in the operator. To gain more insight into this problem, we can think of a perturbational approach for the difference of the effective non-adiabatic Hamiltonians in different embeddings or a comparison of effective rotational models.

Second, if we recall the derivation of the classical Hamiltonian and its quantization (for example, Ref. 27 shows this procedure in our own work), one may ask if it is a good idea to introduce the different rotational and vibrational masses in the Hamiltonian. Although this has been the common practice in these types of phenomenological non-adiabatic models, one might argue that the different masses should be better introduced in the Lagrangian. (In our notation, this means that one has to construct a composite $\boldsymbol{g}$ matrix similar to the composite $\mathcal{G}$ matrix introduced in Eq. (13). Then, this composite $\boldsymbol{g}$ matrix would be inverted to obtain $\mathcal{G}$ instead of using Eq. (13).)

These questions can probably be answered by carrying out the full derivation of the effective Hamiltonians in the spirit of Bunker and Moss for di- and triatomics,[14,19] of Schwenke for H_2O,[20] or most recently of Pachucki and Komasa for diatomic molecules.[15,16] The derivation for polyatomic molecules is probably more complicated than for diatomics, but it properly includes the non-adiabatic mass effects in the rovibrational coupling terms from the beginning. Finally, we note that either case can be accounted for in the non-adiabatic extension of the GENIUSH program reported in this paper, since all the required quantities can be evaluated explicitly over a grid in an automated and numerical approach.

VI. SUMMARY AND CONCLUSION

Second-order rovibrational non-adiabatic effects can be understood as mass effects corresponding to the simple picture that a fraction of the electrons follow the rotating-vibrating atomic nuclei, hence increasing their effective masses.[21] NAPT[15,19] provides a rigorous ground for the derivation of such motion-dependent effective mass functions. To a good level of approximation the rotational mass function can often be replaced with a constant nuclear mass value. At the same time, the vibrational mass function differs more from the nuclear mass and can be derived either from NAPT or from a recent simple, intuitive approach based on the standard Mulliken population analysis of electronic structure theory.[22]

In either case, the direct solution of the rovibrational Schrödinger equation with mass surfaces has not been possible for polyatomic systems. Thus, the purpose of the present work was the extension of the GENIUSH protocol and code so that the rovibrational Schrödinger equation can be solved with motion-dependent mass surfaces.

First, we have considered the case of constant but motion-dependent, rotational and vibrational, masses for the H_3^+ molecular ion. We noticed that the computed rovibrational energy levels are dependent upon the embedding of the body-fixed frame. Among the tested embeddings it was only the Eckart embedding with a symmetric triangular reference structure [Eckart(D_{3h})], which remained invariant under the permutation of the protons. Except for this case of a permutationally invariant embedding, an artificial splitting appeared in the computed degenerate rovibrational eigenvalues. The artificial splitting of the degenerate levels and the deviation from the Eckart(D_{3h}) results increases with the value of the rotational quantum number J, and already for $J = 5$ the deviation was on the order of the expected non-adiabatic correction itself. These numerical observations suggested that if motion-dependent (different rotational and vibrational) masses are used, the eigenvalues are sensitive to the correct permutational symmetry of the embedding of the body-fixed frame, which, interestingly, does not manifest itself if the rotational and vibrational masses are identical.

Next, we employed an Eckart(D_{3h}) embedding, providing the expected degeneracies for the rovibrational states of H_3^+, and optimized the vibrational mass with respect to 15

recently measured high-accuracy transitions,[36,37] while keeping the rotational mass equal to the nuclear mass of the proton. The optimal value of the vibrational mass is larger than the nuclear mass of the proton by about one third of an electron mass, $m^{(v)}_{\mathrm{opt,p}} = m_{\mathrm{nuc,p}} + 0.31224\, m_{\mathrm{e}}$. Using this optimal value the root-mean-square deviation of the computed transitions from the experimental ones is reduced by an order of magnitude compared to the results obtained with Moss' mass. The Moss mass, $m_{\mathrm{Moss,\,p}} = m_{\mathrm{nuc,\,p}} + 0.47531\, m_{\mathrm{e}}$, is the optimal vibrational mass value for the protons in H_2^+[23] but it has been used for modelling second-order non-adiabatic effects also in H_3^+.[11,24] Our optimized value for the vibrational mass is in excellent agreement with the vibrational mass predicted in an iterative approach for the lowest-lying vibrational states with the core-mass surface of Ref. 22. This good agreement is intriguing, since the core-mass surface has been constructed based on a simple Mulliken population analysis.[22]

Last, the implementation of internal-coordinate-dependent mass surfaces in the GENIUSH protocol was investigated. The direct solution of the rovibrational Schrödinger equation with CDMS is thus possible and the developments are awaiting for real-life applications. A good candidate would be the application of the mass surfaces of Ref. 22. On one hand, the proposed direct solution of the rovibrational Schrödinger equation allows to test the validity of the self-consistent iterative approach employed in Ref. 22. On the other hand, it opens the route toward a systematic improvement of the theoretical description of second-order non-adiabatic effects in polyatomic molecules, a significant development for computational molecular spectroscopy.

ACKNOWLEDGMENTS

The financial support of the Hungarian Scientific Research Fund (OTKA, NK83583) is gratefully acknowledged. The computing facilities of NIIF in Debrecen were used during this work.

[1] Y. Suzuki and K. Varga, *Stochastic Variational Approach to Quantum-mechanical Few-body Problems* (Springer-Verlag, Berlin, 1998).
[2] M. Cafiero, S. Bubin, and L. Adamowicz, Phys. Chem. Chem. Phys. **5**, 1491 (2003).
[3] S. Bubin, M. Pavanello, W.-C. Tung, K. L. Sharkey, and L. Adamowicz, Chem. Rev. **113**, 36 (2013).
[4] J. Mitroy, S. Bubin, W. Horiuchi, Y. Suzuki, L. Adamowicz, W. Cencek, K. Szalewicz, J. Komasa, D. Blume, and K. Varga, Rev. Mod. Phys. **85**, 693 (2013).
[5] E. Mátyus and M. Reiher, J. Chem. Phys. **137**, 024104 (2012).
[6] B. Simmen, E. Mátyus, and M. Reiher, Mol. Phys. **111**, 2086 (2013).
[7] E. Mátyus, J. Phys. Chem. A **117**, 7195 (2013).
[8] A. G. Császár, W. D. Allen, Y. Yamaguchi, and H. F. Schaefer III, in *Computational Molecular Spectroscopy*, edited by P. Jensen, and P. R. Bunker (Wiley, Chichester, 2000), pp. 15–68.
[9] O. L. Polyansky, A. G. Császár, S. V. Shirin, N. F. Zobov, P. Barletta, J. Tennyson, D. W. Schwenke, and P. J. Knowles, Science **299**, 539 (2003).
[10] G. Tarczay, A. G. Császár, W. Klopper, and H. M. Quiney, Mol. Phys. **99**, 1769 (2001).
[11] M. Pavanello, L. Adamowicz, A. Alijah, N. F. Zobov, I. I. Mizus, O. L. Polyansky, J. Tennyson, T. Szidarovszky, A. G. Császár, M. Berg *et al.*, Phys. Rev. Lett. **108**, 023002 (2012).
[12] M. Pavanello, L. Adamowicz, A. Alijah, N. F. Zobov, I. I. Mizus, O. L. Polyansky, J. Tennyson, T. Szidarovszky, and A. G. Császár, J. Chem. Phys. **136**, 184303 (2012).
[13] T. Furtenbacher, T. Szidarovszky, E. Mátyus, C. Fábri, and A. G. Császár, J. Chem. Theory Comput. **9**, 5471 (2013).
[14] P. R. Bunker and R. E. Moss, Mol. Phys. **33**, 417 (1977).
[15] K. Pachucki and J. Komasa, J. Chem. Phys. **129**, 034102 (2008).
[16] K. Pachucki and J. Komasa, J. Chem. Phys. **130**, 164113 (2009).
[17] K. Piszczatowski, G. Lach, M. Przybytek, J. Komasa, K. Pachucki, and B. Jeziorski, J. Chem. Theory Comput. **5**, 3039 (2009).
[18] K. Pachucki and J. Komasa, Phys. Chem. Chem. Phys. **12**, 9188 (2010).
[19] P. R. Bunker and R. E. Moss, J. Mol. Spectrosc. **80**, 217 (1980).
[20] D. W. Schwenke, J. Phys. Chem. A **105**, 2352 (2001).
[21] W. Kutzelnigg, Mol. Phys. **105**, 2627 (2007).
[22] L. G. Diniz, J. R. Mohallem, A. Alijah, M. Pavanello, L. Adamowicz, O. L. Polyansky, and J. Tennyson, Phys. Rev. A **88**, 032506 (2013).
[23] R. E. Moss, Mol. Phys. **89**, 195 (1996).
[24] O. L. Polyansky and J. Tennyson, J. Chem. Phys. **110**, 5056 (1999).
[25] R. Jaquet and T. Carrington Jr., J. Phys. Chem. A **117**, 9493 (2013).
[26] A. G. Császár, C. Fábri, T. Szidarovszky, E. Mátyus, T. Furtenbacher, and G. Czakó, Phys. Chem. Chem. Phys. **14**, 1085 (2012).
[27] E. Mátyus, G. Czakó, and A. G. Császár, J. Chem. Phys. **130**, 134112 (2009).
[28] C. Fábri, E. Mátyus, and A. G. Császár, J. Chem. Phys. **134**, 074105 (2011).
[29] J. Echave and D. C. Clary, Chem. Phys. Lett. **190**, 225 (1992).
[30] H. Wei and J. T. Carrington, J. Chem. Phys. **97**, 3029 (1992).
[31] V. Szalay, G. Czakó, A. Nagy, T. Furtenbacher, and A. G. Császár, J. Chem. Phys. **119**, 10512 (2003).
[32] T. Szidarovszky, A. G. Császár, and G. Czakó, Phys. Chem. Chem. Phys. **12**, 8373 (2010).
[33] C. Fábri, E. Mátyus, and A. G. Császár, Spectrochim. Acta **119**, 84 (2014).
[34] See supplementary material at http://dx.doi.org/10.1063/1.4897566 for the detailed numerical results used for Figure 1 and Table I.
[35] C. M. Lindsay and B. J. McCall, J. Mol. Spectrosc. **210**, 60 (2001).
[36] K.-Y. Wu, Y.-H. Liena, C.-C. Liao, Y. R. Lin, and J.-T. Shy, Phys. Rev. A **88**, 032507 (2013).
[37] J. N. Hodges, A. J. Perry, P. A. Jenkins, B. M. Siller, and B. J. McCall, J. Chem. Phys. **139**, 164201 (2013).
[38] The center of mass is at the origin. The three protons are in the *xy* plane. The *x*-axis is parallel to the displacement vector between proton-1 and proton-2, and proton-3 has a non-negative *y* coordinate value.